Electronic Supplementary Information

Ruthenium nitrosyl complexes with 1,4,7-trithiacyclononane and 2,2′-bipyridine (bpy) or 2-phenylazopyridine (pap) coligands. Electronic structure and reactivity aspects

Prinaka De,[a] Somnath Maji,[a] Abhishek Dutta Chowdhury,[a] Shaikh M. Mobin,[a] Tapan Kumar Mondal,[b] Alexa Paretzki[c] and Goutam Kumar Lahiri[*a]

[a] *Department of Chemistry, Indian Institute of Technology Bombay, Powai, Mumbai 400076, India, E-mail: lahiri@chem.iitb.ac.in*

[b] *Department of Chemistry, Jadavpur University, Jadavpur, Kolkata-700032, India*

[c] *Institut für Anorganische Chemie, Universität Stuttgart, Pfaffenwaldring 55, D-70550 Stuttgart, Germany*

Table S1 Crystallographic data for $[Ru^{II}([9]aneS_3)(bpy)(NO_2)](ClO_4)$ [**3**](ClO_4), $[Ru^{II}([9]aneS_3)(pap)(Cl)](ClO_4)$ [**5**](ClO_4), $[Ru^{II}([9]aneS_3)(pap)(CH_3CN)](ClO_4)_2$ [**6**]$(ClO_4)_2$, $[Ru^{II}([9]aneS_3)(pap)(NO_2)](ClO_4)$ [**7**](ClO_4)

	[**3**](ClO_4)	[**5**](ClO_4)	[**6**]$(ClO_4)_2$	[**7**](ClO_4)
Empirical formula	$C_{16}H_{20}ClN_3O_6S_3Ru$	$C_{17}H_{21}Cl_2N_3O_4S_3Ru$	$C_{19}H_{24}Cl_2N_4O_8S_3Ru$	$C_{17}H_{21}ClN_4O_6S_3Ru$
M_r	583.05	599.52	704.57	610.08
Temperature	150(2) K	120(2) K	120(2) K	120(2) K
Crystal symmetry	Monoclinic	Monoclinic	Monoclinic	Monoclinic
space group	*P* 21/c	*C* 2/c	*P* 21/c	*P* 21/c
a/Å	13.9612(3)	25.0741(6)	19.033(2)	11.5192(9)
b/Å	10.3777(2)	11.9072(2)	9.4724(9)	23.074(2)
c/Å	13.9987(2)	16.1053(3)	15.2998(16)	8.5728(9)
α/°	90	90	90	90
β/°	92.437(2)	112.209(3)	111.793(12)	93.618(8)
γ/°	90	90	90	90
V /Å^3	2026.37(7)	4451.70(15)	2561.2(5)	2274.0(4)
Z	4	8	4	4
D_{calcd} (g cm^{-3})	1.911	1.789	1.827	1.782
μ(mm^{-1})	1.256	1.256	1.119	1.125
F(000)	1176	2416	1424	1232
2θ range(deg)	7.02 to 49.98	6 to 50	5.88 to 50	5.92 to 49.98
Data / restraints / parameters	3567 / 0 / 271	3919 / 0 / 271	4504 / 0 / 335	4004 / 0 / 289
GOF	1.064	1.057	0.941	1.272
R1, wR2 [$I > 2\sigma(I)$]	0.0182, 0.0475	0.0406, 0.1004	0.0501, 0.0899	0.0397, 0.0750
R1, wR2(all data)	0.0203, 0.0481	0.0561, 0.1047	0.0936, 0.1006	0.0444, 0.0886
Largest diff. Peak/hole, (e Å^{-3})	0.420, −0.382	1.560, -1.434	1.167, -0.732	1.192, -0.977

Table S2 Selected bond distances (Å) and bond angles (°) for $[Ru^{II}([9]aneS_3)(bpy)(NO_2)](ClO_4)$ [**3**](ClO_4), $[Ru^{II}([9]aneS_3)(pap)(Cl)](ClO_4)$ [**5**](ClO_4), $[Ru^{II}([9]aneS_3)(pap)(CH_3CN)](ClO_4)_2$ [**6**]$(ClO_4)_2$, $[Ru^{II}([9]aneS_3)(pap)(NO_2)](ClO_4)$ [**7**](ClO_4)

Distances/angles	[**3**](ClO_4) (X=NO_2)	[**5**](ClO_4) (X=Cl)	[**6**]$(ClO_4)_2$ (X=CH_3CN)	[**7**](ClO_4) (X=NO_2)
Ru(1)-N(1)	2.0823(15)	2.069(4)	2.073(5)	2.066(3)
Ru(1)-N(2)	2.0875(16)	1.998(4)	2.030(5)	2.037(3)
Ru(1)-S(1)	2.3084(5)	2.3402(13)	2.3426(16)	2.3353(10)
Ru(1)-S(2)	2.3012(5)	2.3308(12)	2.3283(16)	2.3298(10)
Ru(1)-S(3)	2.3435(5)	2.2980(13)	2.3152(15)	2.3404(11)
Ru(1)-X	2.0605(16)	2.4055(12)	2.062(5)	2.084(4)
X-O(1)	1.248(2)	-	-	1.237(4)
X-O(2)	1.248(2)	-	-	1.232(5)
N(2)-N(3)	-	1.287(5)	1.287(6)	1.284(5)
S(1)-Ru(1)-S(2)	87.548(17)	87.18(4)	87.39(6)	87.21(3)
S(1)-Ru(1)-S(3)	87.984(17)	88.00(5)	87.62(6)	87.75(4)
S(2)-Ru(1)-S(3)	88.456(16)	87.92(4)	87.82(6)	87.80(4)
N(1)-Ru(1)-S(2)	174.07(4)	174.92(11)	173.91(13)	174.22(10)
N(1)-Ru(1)-N(2)	78.17(6)	75.72(15)	75.52(18)	76.25(13)
N(1)-Ru(1)-S(1)	97.69(4)	97.40(11)	98.41(13)	97.45(9)
N(2)-Ru(1)-S(1)	175.86(4)	173.09(11)	173.90(14)	173.66(9)
N(1)-Ru(1)-S(3)	88.97(4)	94.39(11)	90.53(12)	88.94(10)
N(2)-Ru(1)-S(2)	96.58(4)	99.72(11)	98.67(13)	99.05(9)
N(2)-Ru(1)-S(3)	91.85(4)	91.81(11)	91.92(13)	91.43(10)
N(1)-Ru(1)-X	89.90(6)	88.45(11)	91.46(18)	89.66(14)
N(2)-Ru(1)-X	87.82(6)	95.27(11)	91.55(18)	93.80(13)
S(1)-Ru(1)-X	92.27(5)	85.11(5)	89.06(14)	86.75(9)
S(2)-Ru(1)-X	92.66(4)	89.78(4)	90.51(14)	94.05(9)
S(3)-Ru(1)-X	178.86(4)	172.84(5)	176.34(14)	174.10(9)
O(1)-X-O(2)	118.47(16)	-	-	119.8(4)
Ru(1)-N(4)-C(18)	-	-	173.5(5)	-
N(4)-C(18)-C(19)	-	-	177.9(6)	-

Table S3 Conformations of coordinated [9]aneS_3 in the crystal structures based on the endocyclic torsion angles around the macrocyclic ring

	3^{+}	**4**$^{3+}$
C(16)-S(1)-C(11)-C(12)	67.12(15)	60.2(5)
S(1)-C(11)-C(12)-S(2)	47.97(17)	52.7(5)
C(13)-S(2)-C(12)-C(11)	-135.19(14)	-134.0(4)
C(12)-S(2)-C(13)-C(14)	64.47(15)	63.2(4)
S(2)-C(13)-C(14)-S(3)	50.12(17)	50.1(5)
C(15)-S(3)-C(14)-C(13)	-134.16(14)	-132.2(4)
C(14)-S(3)-C(15)-C(16)	63.89(16)	62.7(5)
S(3)-C(15)-C(16)-S(1)	48.56(18)	52.8(5)
C(11)-S(1)-C(16)-C(15)	-135.15(14)	-135.1(4)

	5^{+}	**6**$^{2+}$	**7**$^{+}$
C(17)-S(1)-C(12)-C(13)	-66.1(5)	-67.7(6)	64.8(3)
S(1)-C(12)-C(13)-S(2)	-48.4(5)	-45.7(7)	48.8(4)
C(14)-S(2)-C(13)-C(12)	135.1(4)	130.9(5)	-134.9(3)
C(13)-S(2)-C(14)-C(15)	-67.0(5)	-67.1(6)	67.4(4)
S(2)-C(14)-C(15)-S(3)	-46.7(5)	-49.3(7)	45.9(4)
C(16)-S(3)-C(15)-C(14)	133.5(5)	135.8(5)	-131.0(3)
C(15)-S(3)-C(16)-C(17)	-66.5(4)	-64.5(5)	63.9(4)
S(3)-C(16)-C(17)-S(1)	-47.1(5)	-46.9(6)	51.4(4)
C(12)-S(1)-C(17)-C(16)	133.1(4)	131.7(5)	-137.1(3)

Table S4 DFT calculated selective bond distances and bond angles for $[Ru^{II}([9]aneS_3)(pap)(NO)]^{3+}$ (**8**$^{3+}$) and $[Ru^{II}([9]aneS_3)(pap)(NO)]^{2+}$ (**8**$^{2+}$)

	8^{3+}	**8**$^{2+}$
Ru(1)-N(1)	2.114	2.106
Ru(1)-N(2)	2.162	2.136
Ru(1)-N(4)	1.749	1.911
Ru(1)-S(1)	2.462	2.418
Ru(1)-S(2)	2.454	2.426
Ru(1)-S(3)	2.460	2.449
N(4)-O(1)	1.135	1.165
N(2)-N(3)	1.269	1.270
N(1)-Ru(1)-N(2)	75.99	75.59
N(1)-Ru(1)-N(4)	94.399	89.19
N(1)-Ru(1)-S(1)	96.819	96.80
N(1)-Ru(1)-S(2)	170.3	175.9
N(1)-Ru(1)-S(3)	85.60	91.23
N(2)-Ru(1)-N(4)	94.13	92.29
N(2)-Ru(1)-S(1)	168.9	170.9
N(2)-Ru(1)-S(2)	100.6	101.4
N(2)-Ru(1)-S(3)	85.86	89.08
N(4)-Ru(1)-S(1)	94.81	92.40
N(4)-Ru(1)-S(2)	94.93	93.65
N(4)-Ru(1)-S(3)	180.0	178.6
S(1)-Ru(1)-S(2)	85.10	85.98
S(1)-Ru(1)-S(3)	85.18	86.24
S(2)-Ru(1)-S(3)	85.06	85.99
Ru(1)-N(4)-O(1)	179.2	139.4

Table S5 DFT calculated conformational analysis of $\mathbf{4}^{2+}$ and $\mathbf{8}^{2+}$

	$\mathbf{4}^{2+}$	$\mathbf{8}^{2+}$
Optimized	-985.93942540 ($\theta = 4.45°$)	-1079.34692984 ($\theta = 0.41°$)
Eclipsed ($\theta = 0°$)[a]	-985.93904358	-1079.34571773
Staggered ($\theta = 45°$)[a]	-985.93824075	-1079.34514831
ΔE(optimized-eclipsed)[b]	-0.2396 kcal/mol (83.8 cm^{-1})	-0.7606 kcal/mol (266.0 cm^{-1})
ΔE(optimized-staggered)[b]	-0.7434 kcal/mol (260.0 cm^{-1})	-1.1179 kcal/mol (391.0 cm^{-1})

[a]Energy in Hartrees.

[b]Energy in kcal/mol and cm^{-1}.

Table S6 ^{1}H NMR spectral data in CD_3CN

Complex	δ, ppm (*J*, Hz)	
	Aromatic protons	Aliphatic protons
2^{2+}	8.93 (5.2) (d, 2H) 8.47 (8.1) (d, 2H) 8.20 (8.0, 7.8) (t, 2H) 7.67 (6.6) (t, 2H)	3.03-2.89 (4H) 2.84-2.67 (4H) 2.62-2.46 (4H) 2.13 (3H) (CH_3CN)
3^{+}	9.00 (5.2) (d, 2H) 8.43 (8.0) (d, 2H) 8.14 (7.9, 7.8) (t, 2H) 7.60 (6.6) (t, 2H)	3.20-3.09 (2H) 2.95-2.85 (2H) 2.76-2.63 (4H) 2.60-2.42 (4H)
4^{3+}	8.91 (5.5) (d, 2H) 8.75 (8.2) (d, 2H) 8.60 (8.0, 7.9) (t, 2H) 8.03 (6.7) (t, 2H)	3.95-3.84 (4H) 3.70-3.59 (4H) 3.48-3.38 (4H)
5^{+}	9.13 (5.4) (d, 1H) 8.68 (8.1) (d, 1H) 8.25 (7.9) (t, 1H) 7.83 (m, 2H) 7.78 (9.0, 6.0) (t, 1H) 7.64 (3.9, 2.7) (t, 3H)	3.38-3.14 (4H) 3.10-2.98 (2H) 2.88-2.68 (2H) 2.66-2.54 (1H) 2.54-2.42 (1H) 2.40-2.20 (2H)
6^{2+}	9.09 (5.4) (d, 1H) 8.81 (8.1) (d, 1H) 8.43 (9.0, 6.0) (t, 1H) 7.92 (6.9, 5.4) (t, 1H) 7.83 (9.0) (d, 2H) 7.72 (m, 3H)	3.40-3.18 (3H) 3.02-2.86 (2H) 2.84-2.72 (2H) 2.66-2.44 (3H) 2.42-2.26 (2H) 2.23 (3H) (CH_3CN)
7^{+}	9.12 (6.0) (d, 1H) 8.77 (6.0) (d, 1H) 8.35 (9.0) (t, 1H) 7.82 (6.6) (t, 1H) 7.76 (m, 2H) 7.66 (m, 3H)	3.44-3.30 (2H) 3.22-3.12 (2H) 3.04-2.92 (1H) 2.82-2.73 (1H) 2.62-2.38 (4H) 2.36-2.24 (2H)
8^{3+}	9.20 (7.5) (d, 1H) 9.13 (5.4) (d, 1H) 8.89 (7.8) (t, 1H) 8.30 (6.3, 6.0) (t, 1H) 8.09 (9.0) (d, 2H) 8.00 (7.5, 7.2) (t, 1H) 7.85 (8.4, 7.5) (t, 2H)	4.04-3.96 (1H) 3.94-3.82 (3H) 3.78-3.60 (4H) 3.58-3.46 (1H) 3.42-3.26 (2H) 2.82-2.66 (1H)

Table S7 ^{13}C NMR spectral data in CD_3CN

Complex	δ, ppm	
	Aromatic carbons	Aliphatic carbons
3^{+}	157.92 154.53 139.61 128.31 124.64	33.91 33.79 32.82
4^{3+}	157.23 156.47 145.83 131.95 127.95	40.74 40.39 38.56
7^{+}	166.36 157.99 152.68 141.56 132.89 130.59 129.96 129.59 123.65	36.87 36.30 34.67 32.77 32.56 32.05
8^{3+}	166.30 157.94 152.67 141.55 132.87 130.58 129.97 129.59 123.62	36.84 36.29 34.65 32.69 32.50 31.97

Table S8 Electronic spectral data in CH_3CN

Complex	λ/nm (ε / M^{-1} cm^{-1})
$\mathbf{2}^{2+}$	384(2280), 315(4080), 307(4680), 278(13010), 240(6400)
$\mathbf{3}^{+}$	408(1300), 316(2120), 283(12450), 241(7690)
$\mathbf{4}^{3+}$	306(6490), 226(17580)
$\mathbf{4}^{2+}$	407(1790), 315(3400), 285(10760), 242(7260)
$\mathbf{5}^{+}$	534(4180), 367(4120), 316(8760)
$\mathbf{6}^{2+}$	480(5450), 369(7260), 306(6700), 278(7940)
$\mathbf{7}^{+}$	498(5190), 363(7160), 309(9330), 281(8360)
$\mathbf{8}^{3+}$	444(2750), 358(4370), 311(4190), 275(4370)
$\mathbf{8}^{2+}$	500(3260), 343(5590), 315(5920), 282(5090)

Table S9(a) TD-DFT results for $[Ru^{II}([9]aneS_3)(bpy)(NO^+)]^{3+}$ ($\mathbf{4}^{3+}$)

Excitation energy/eV	λ/nm	f	Transition	Character
3.09	400.9	0.0048	(64%)HOMO-2 → LUMO	bpy(π) → NO(π^*)/Ru(dπ)
3.20	387.3	0.0057	(67%)HOMO-4 → LUMO	L(π)/bpy(π)→NO(π^*)/Ru(dπ)
3.91	317.1	0.0908	(69%)HOMO → LUMO+4	bpy(π) → bpy(π^*)
4.04	306.8	0.0316	(53%)HOMO-4→LUMO+2 (21%)HOMO-3 → LUMO+3	L(π)/bpy(π) → Ru(dπ)
4.47	277.2	0.0305	(45%)HOMO-5 → LUMO+4 (24%)HOMO-5 → LUMO+5	bpy(π) → bpy(π^*)
4.49	275.9	0.0204	(43%)HOMO-5 → LUMO+5 (23%)HOMO-5 → LUMO+4	bpy(π) → bpy(π^*)

Table S9(b) TD-DFT Results for $[Ru^{II}([9]aneS_3)(pap)(NO^+)]^{3+}$ ($\mathbf{8}^{3+}$)

Excitation energy/ eV	λ/nm	f	Transition	Character
2.70	459.2	0.0432	(61%)HOMO-1 → LUMO+1 (21%)HOMO → LUMO	pap(π) → NO(π^*)/Ru(dπ)
2.84	435.6	0.0789	(67%)HOMO-2 → LUMO	pap(π) → NO(π^*)/Ru(dπ)
3.38	366.9	0.0883	(89%)HOMO → LUMO+4	pap(π) → pap(π^*)
3.51	352.8	0.0556	(63%)HOMO-2 → LUMO+2	pap(π) → pap(π^*)
4.23	292.7	0.0913	(45%)HOMO-7 → LUMO+2 (37%)HOMO-6 → LUMO+2	pap(π)/L(π) → pap(π^*)

Table S10(a) TD-DFT results for $[Ru^{II}([9]aneS_3)(bpy)(NO^{\bullet})]^{2+}$ ($\mathbf{4}^{2+}$)

Excitation energy/eV	λ/nm	f	Transition	Character
2.76	448.8	0.0016	(37%)HOMO-3(α) → LUMO(α) (47%)HOMO-2(β) → LUMO+1(β)	Ru(dπ)/bpy(π)→NO(π^*)
2.92	424.6	0.0045	(56%)HOMO-1(α) → LUMO+1(α)	bpy(π) → bpy(π^*)
3.02	410.2	0.0105	(60%)HOMO(β) → LUMO+2(β)	Ru(dπ) → bpy(π^*)
3.40	364.1	0.0090	(62%)HOMO-3(β) → LUMO+2(β)	Ru(dπ) → bpy(π^*)
3.46	357.9	0.0102	(53%)HOMO-3(α) → LUMO+1(α)	Ru(dπ)/bpy(π) → bpy(π^*)
3.72	333.0	0.0245	(29%)HOMO-4(α) → LUMO+1(α) (28%)HOMO-4(β) → LUMO+2(β)	Ru(dπ)/bpy(π) → bpy(π^*) L(π)/bpy(π)→ bpy(π^*)
3.89	318.5	0.0239	(82%)HOMO-2(β) → LUMO+4(β)	Ru(dπ)/bpy(π) → bpy(π^*)
4.26	290.8	0.0451	(37%)HOMO-7(α) → LUMO+1(α) (25%)HOMO-6(β) → LUMO+2(β)	bpy(π) → bpy(π^*)
4.42	280.1	0.0637	(43%)HOMO-6(β) → LUMO+2(β) (21%)HOMO-7(α) → LUMO+1(α)	bpy(π) → bpy(π^*)

Table S10(b) TD-DFT results for $[Ru^{II}([9]aneS_3)(pap)(NO^{\bullet})]^{2+}$ ($\mathbf{8}^{2+}$)

Excitation energy/eV	λ/nm	f	Transition	Character
2.30	538.5	0.0066	(69%)SOMO(α) → LUMO(α)	Ru(dπ)/NO(π^*) → pap(π^*)
2.55	486.5	0.0159	(43%)HOMO-3(α) → LUMO(α) (26%)HOMO-3(α) → LUMO+1(α)	Ru(dπ) → pap(π^*) Ru(dπ) → NO(π^*)
3.71	334.0	0.0583	(47%)HOMO-5(β) → LUMO(β) (28%)HOMO-6(α) → LUMO(α)	pap(π) → pap(π^*)
3.94	314.5	0.0026	(51%)HOMO-6(β) → LUMO(β) (32%)HOMO-8(α) → LUMO(α)	pap(π)/L(π) → pap(π^*)

Table S11 Redox potential data[a]

	E^{o}_{298}/V (ΔE_p/mV)			
Complex	Ru^{III}/Ru^{II}	$NO^+ \rightarrow NO^\bullet$ (**I**)	$NO^\bullet \rightarrow NO^-$ (**II**)	Ligand reduction
$\mathbf{2}^{2+}$	1.61(70)	–	–	-1.41(70), -1.57(70)
$\mathbf{3}^{+}$	1.31[b]	–	–	-1.55(70), -1.79(70),
$\mathbf{4}^{3+}$	>2	0.49(90)	0.07[b]	-1.01[b], -1.52(70)
$\mathbf{5}^{+}$	1.34(80)	–	–	-0.74(80), -1.30(120), -1.51(70)
$\mathbf{6}^{2+}$	1.86(90)	–	–	-0.49(70), -1.16(130), -1.50(70)
$\mathbf{7}^{+}$	1.68[b]	–	–	-0.52(70), -1.31[b], -1.39[b]
$\mathbf{8}^{3+}$	>2	0.67(90)	0.03[b]	-0.44[b], -0.53(60), -0.71(60)

[a]Potentials with reference to SCE; in CH_3CN/0.1 M Et_4NClO_4; scan rate, 100 mV s^{-1}.

[b]Irreversible.

Table S12 MO composition of $\mathbf{4}^{3+}$

MO	Energy/ eV	Composition			
		Ru	bpy	[9]aneS$_3$	NO
LUMO+5	-10.65	02	91	07	0
LUMO+4	-11.72	05	92	02	01
LUMO+3	-12.18	50	22	28	0
LUMO+2	-12.28	49	12	30	09
LUMO+1	-13.41	22	02	04	72
LUMO	-13.41	24	02	04	70
HOMO	-16.39	01	99	0	0
HOMO-1	-17.49	21	55	18	06
HOMO-2	-17.58	07	85	03	05
HOMO-3	-17.83	30	25	44	01
HOMO-4	-17.92	19	20	55	06
HOMO-5	-17.94	02	74	23	01
HOMO-6	-18.25	10	27	62	01
HOMO-7	-18.46	42	22	31	05
HOMO-8	-18.94	14	58	27	01
HOMO-9	-19.21	46	21	18	15
HOMO-10	-19.28	28	49	19	04

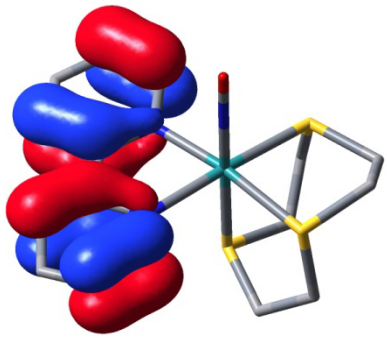

HOMO

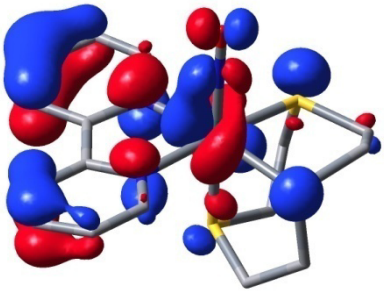

HOMO-1

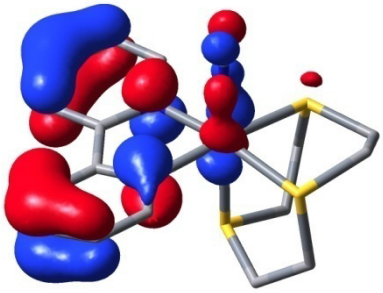

HOMO-2

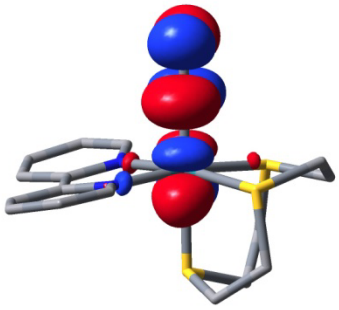

LUMO

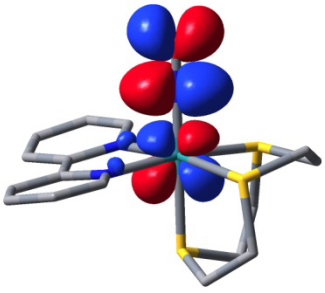

LUMO+1

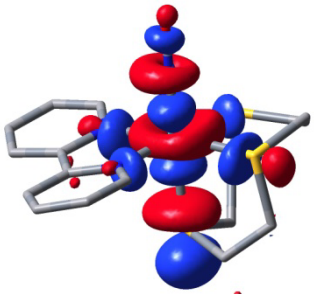

LUMO+2

Table S13 MO composition of $\mathbf{8}^{3+}$

MO	Energy/ eV	Composition			
		Ru	pap	[9]aneS$_3$	NO
LUMO+5	-10.72	50	18	28	04
LUMO+4	-12.18	02	94	04	0
LUMO+3	-12.32	49	17	29	05
LUMO+2	-12.73	08	86	03	03
LUMO+1	-13.43	23	02	04	71
LUMO	-13.46	19	10	03	68
HOMO	-15.62	01	99	0	0
HOMO-1	-15.76	01	98	01	0
HOMO-2	-17.27	04	86	10	0
HOMO-3	-17.43	06	70	21	03
HOMO-4	-17.56	19	55	20	06
HOMO-5	-17.81	25	39	35	01
HOMO-6	-18.02	22	17	57	04
HOMO-7	-18.21	03	81	15	01
HOMO-8	-18.26	13	31	52	04
HOMO-9	-18.46	02	92	05	01
HOMO-10	-18.58	35	34	27	04

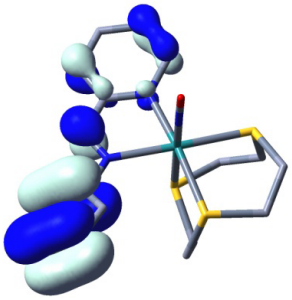

HOMO

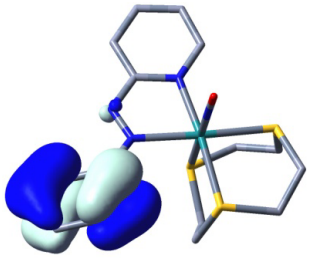

HOMO-1

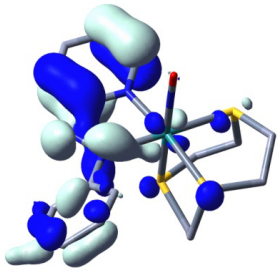

HOMO-2

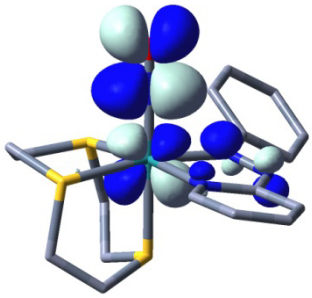

LUMO

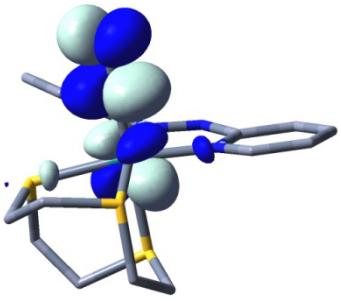

LUMO+1

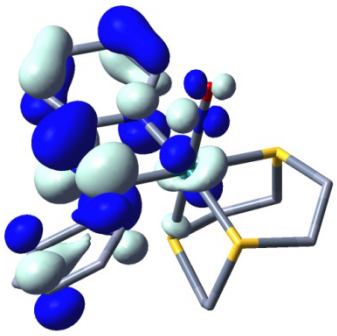

LUMO+2

Table S14a MO composition of $\mathbf{4}^{2+}$

α-spin					
MO	Energy/ eV	Composition			
		Ru	bpy	[9]aneS$_3$	NO
LUMO+5	-7.17	19	65	09	07
LUMO+4	-7.22	26	50	15	09
LUMO+3	-7.35	09	81	07	03
LUMO+2	-7.62	52	18	30	0
LUMO+1	-8.33	03	96	01	0
LUMO	-8.96	17	01	04	78
SOMO	-12.03	30	05	12	53
HOMO-1	-13.06	04	95	01	0
HOMO-2	-13.21	70	05	20	05
HOMO-3	-13.41	52	24	11	13
HOMO-4	-13.73	51	18	07	24
HOMO-5	-14.27	05	32	63	0

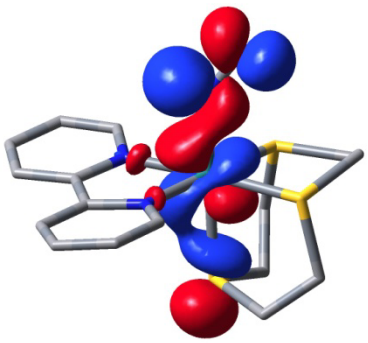

SOMO

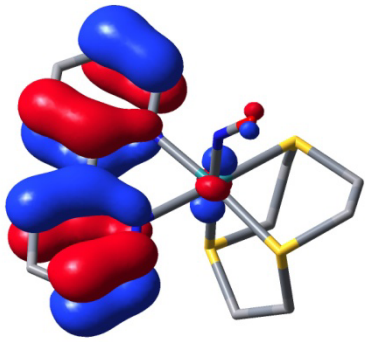

HOMO-1

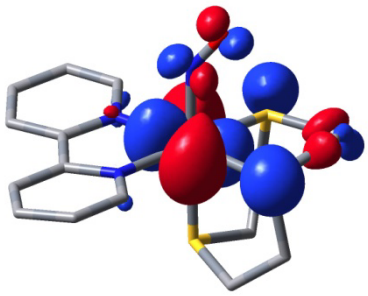

HOMO-2

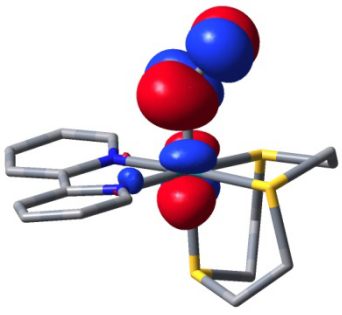

LUMO

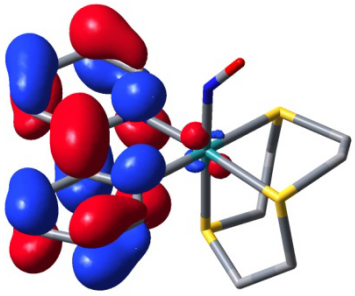

LUMO+1

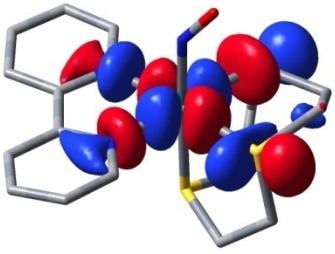

LUMO+2

Table S14b MO composition of $\mathbf{4}^{2+}$

β-spin					
MO	Energy/ eV	Composition			
		Ru	bpy	[9]aneS$_3$	NO
LUMO+5	-7.19	02	95	03	0
LUMO+4	-7.32	02	96	02	0
LUMO+3	-7.57	52	18	30	0
LUMO+2	-8.30	04	93	02	01
LUMO+1	-8.58	14	04	04	78
LUMO	-8.97	28	06	12	54
HOMO	-13.02	62	14	19	05
HOMO-1	-13.05	07	90	02	01
HOMO-2	-13.36	63	17	12	08
HOMO-3	-13.37	70	13	10	07
HOMO-4	-14.27	05	33	62	0
HOMO-5	-14.35	10	14	74	02

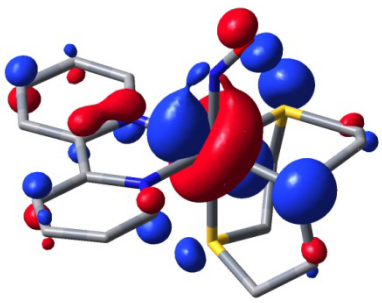

HOMO

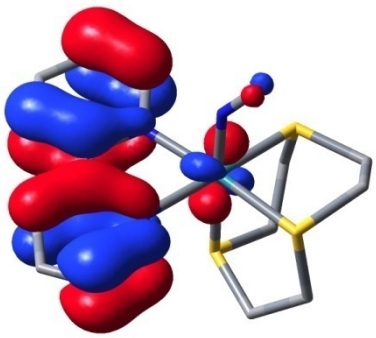

HOMO-1

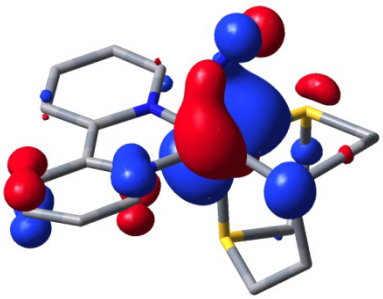

HOMO-2

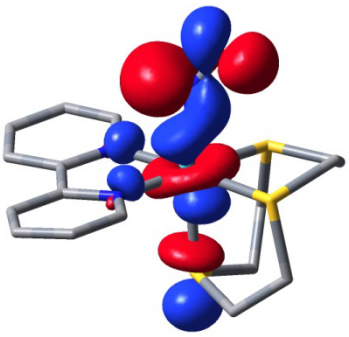

LUMO

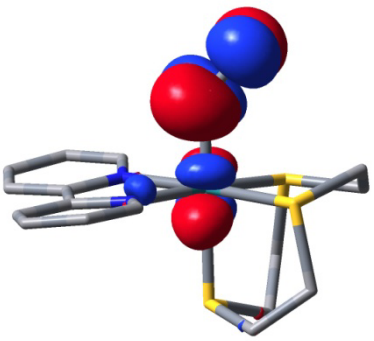

LUMO+1

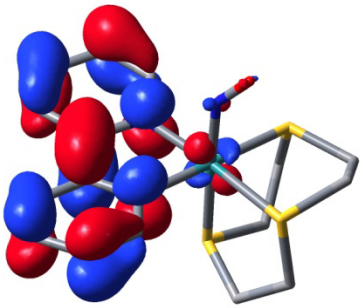

LUMO+2

Table S15a. MO composition of $\mathbf{8}^{2+}$

α-spin					
MO	Energy/ eV	Composition			
		Ru	pap	[9]aneS$_3$	NO
LUMO+5	-6.59	12	18	70	0
LUMO+4	-7.28	49	10	24	17
LUMO+3	-7.41	04	92	03	01
LUMO+2	-7.79	52	18	29	01
LUMO+1	-8.96	19	19	02	60
LUMO	-9.39	02	77	01	20
SOMO	-12.20	31	07	12	50
HOMO-1	-12.54	02	93	01	04
HOMO-2	-12.70	01	98	01	0
HOMO-3	-13.30	62	13	20	05
HOMO-4	-13.58	52	14	23	11
HOMO-5	-13.73	46	28	09	17

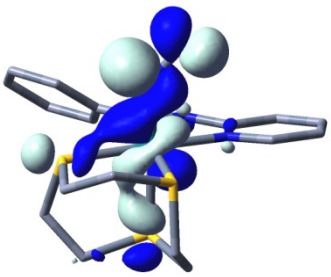

SOMO

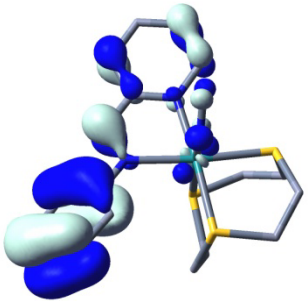

HOMO-1

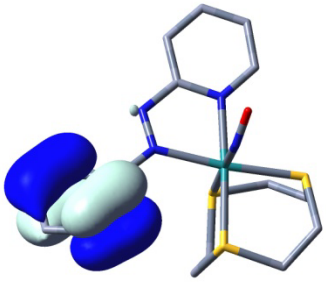

HOMO-2

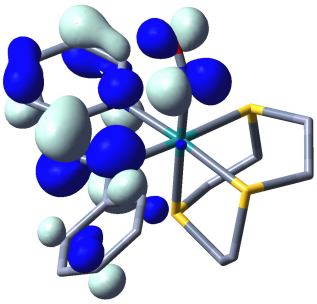

LUMO

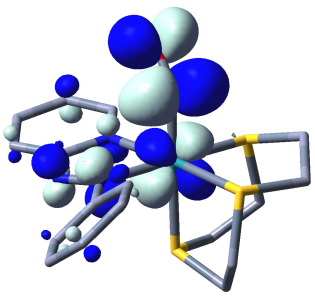

LUMO+1

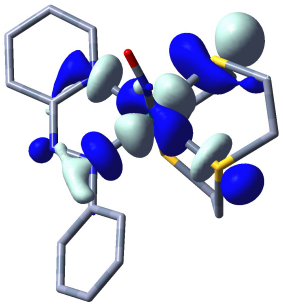

LUMO+2

Table S15b MO composition of $\mathbf{8}^{2+}$

β-spin					
MO	Energy/ eV	Composition			
		Ru	pap	[9]aneS$_3$	NO
LUMO+5	-6.74	34	06	28	32
LUMO+4	-7.40	02	96	02	0
LUMO+3	-7.72	52	18	29	01
LUMO+2	-8.63	17	05	02	76
LUMO+1	-9.13	02	90	01	07
LUMO	-9.33	30	03	13	54
HOMO	-12.52	04	95	01	0
HOMO-1	-12.70	01	98	01	0
HOMO-2	-13.14	57	17	20	06
HOMO-3	-13.32	73	10	14	03
HOMO-4	-13.63	55	21	15	09
HOMO-5	-13.91	06	65	26	03

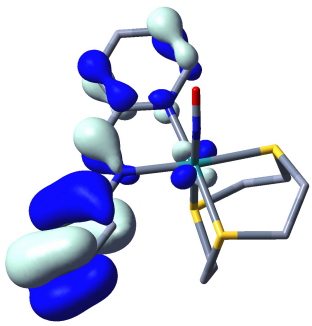

HOMO

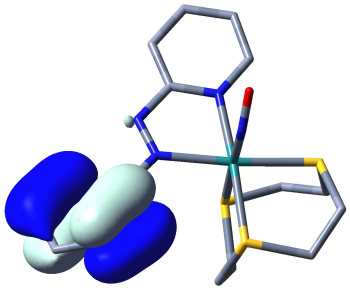

HOMO-1

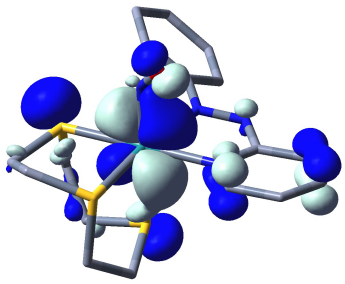

HOMO-2

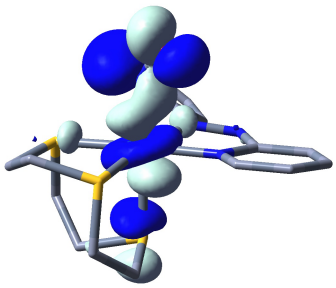

LUMO

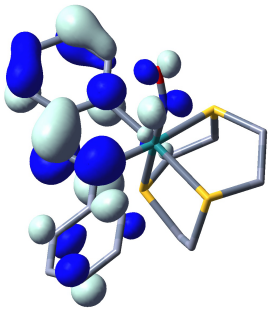

LUMO+1

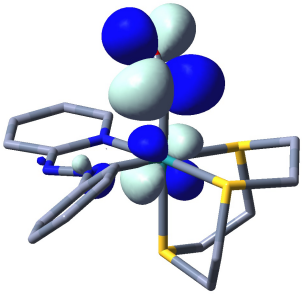

LUMO+2

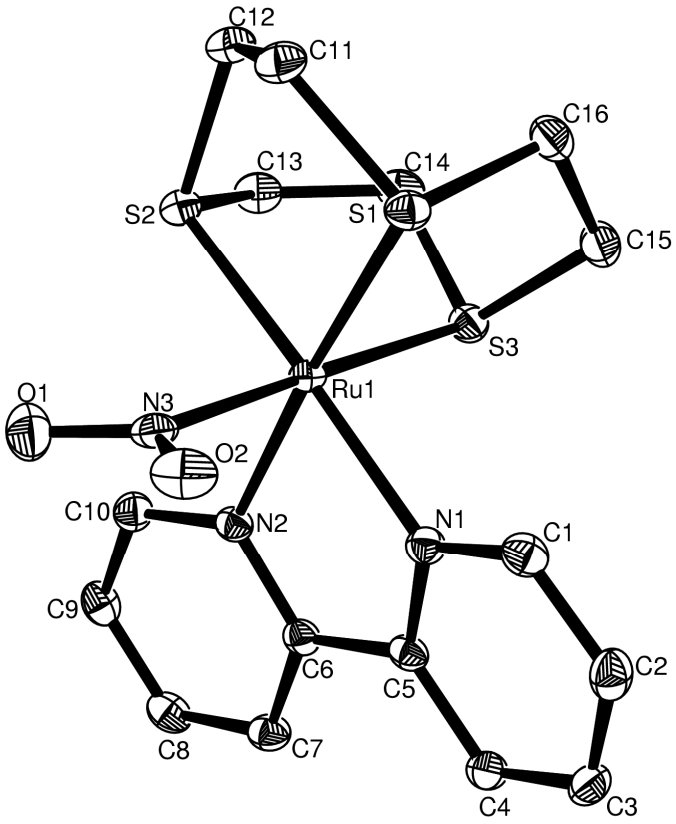

Fig. S1 Molecular structure of the cation of $[Ru^{II}([9]aneS_3)(bpy)(NO_2)](ClO_4)$ in the crystal structure of [**3**](ClO_4). Ellipsoids are drawn at 50% probability. Hydrogen atoms are omitted for clarity.

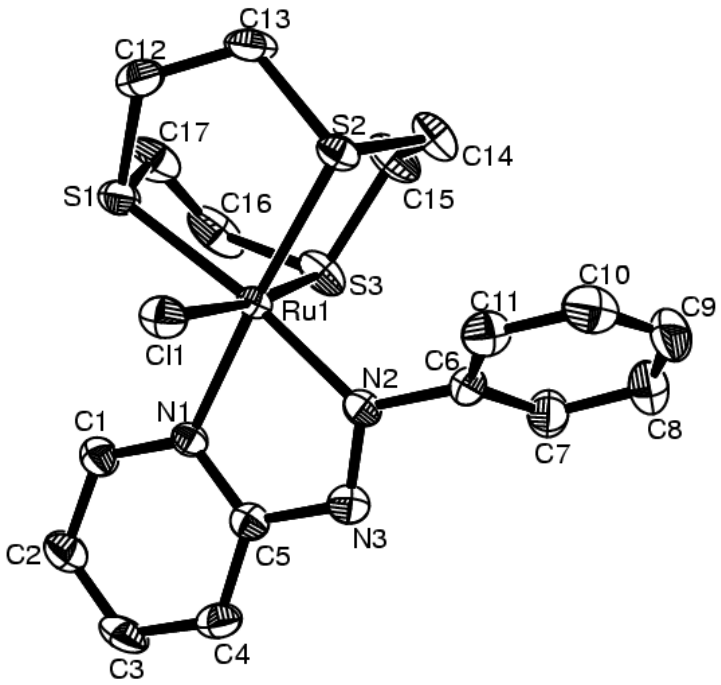

Fig. S2 Molecular structure of the cation of $[Ru^{II}([9]aneS_3)(pap)(Cl)](ClO_4)$ in the crystal structure of [**5**](ClO_4). Ellipsoids are drawn at 50% probability. Hydrogen atoms are omitted for clarity.

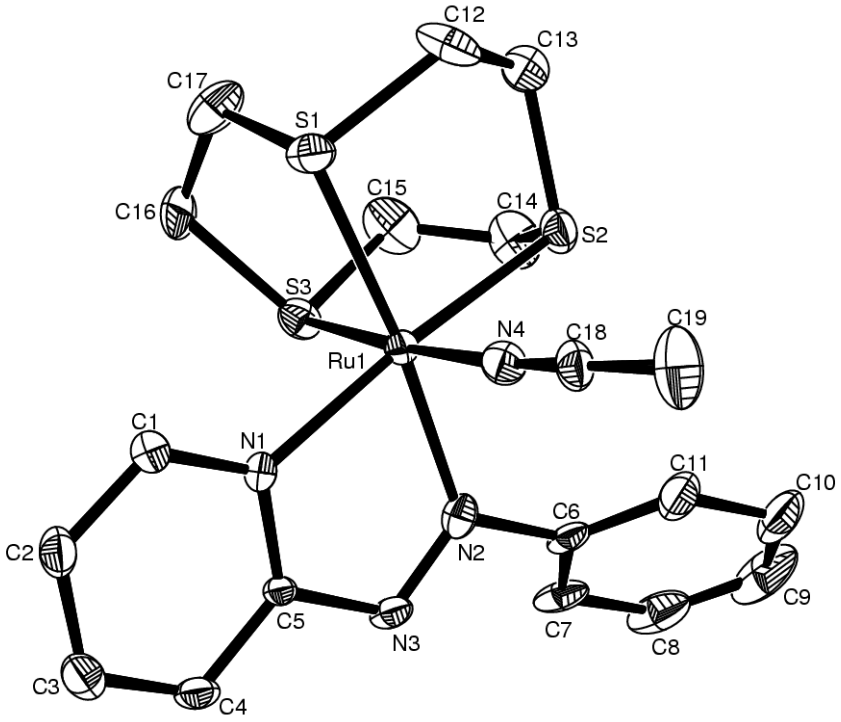

Fig. S3 Molecular structure of the cation of $[Ru^{II}([9]aneS_3)(pap)(CH_3CN)](ClO_4)_2$ in the crystal structure of [**6**]$(ClO_4)_2$. Ellipsoids are drawn at 50% probability. Hydrogen atoms are omitted for clarity.

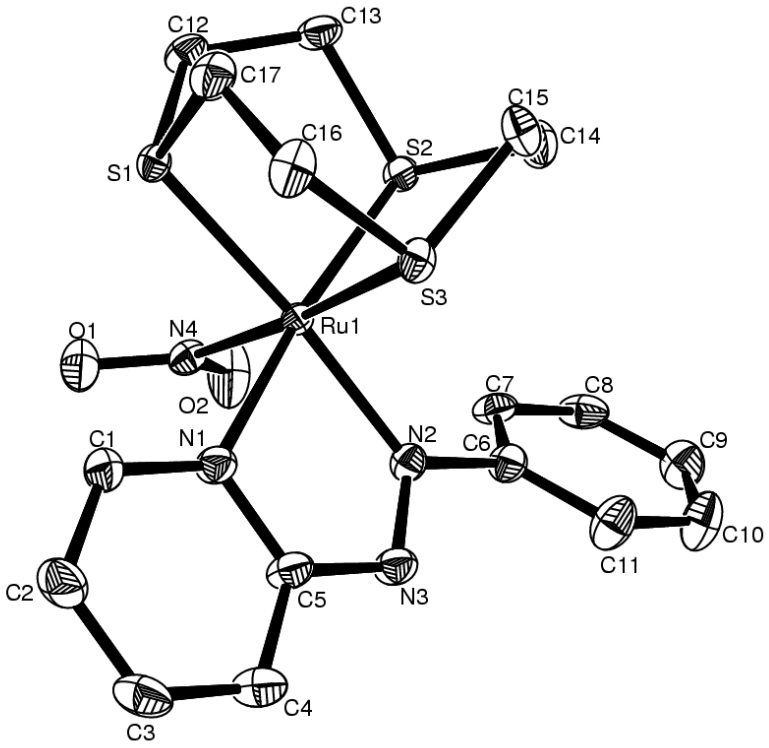

Fig. S4 Molecular structure of the cation of $[Ru^{II}([9]aneS_3)(pap)(NO_2)](ClO_4)$ in the crystal structure of [**7**](ClO_4). Ellipsoids are drawn at 50% probability. Hydrogen atoms are omitted for clarity.

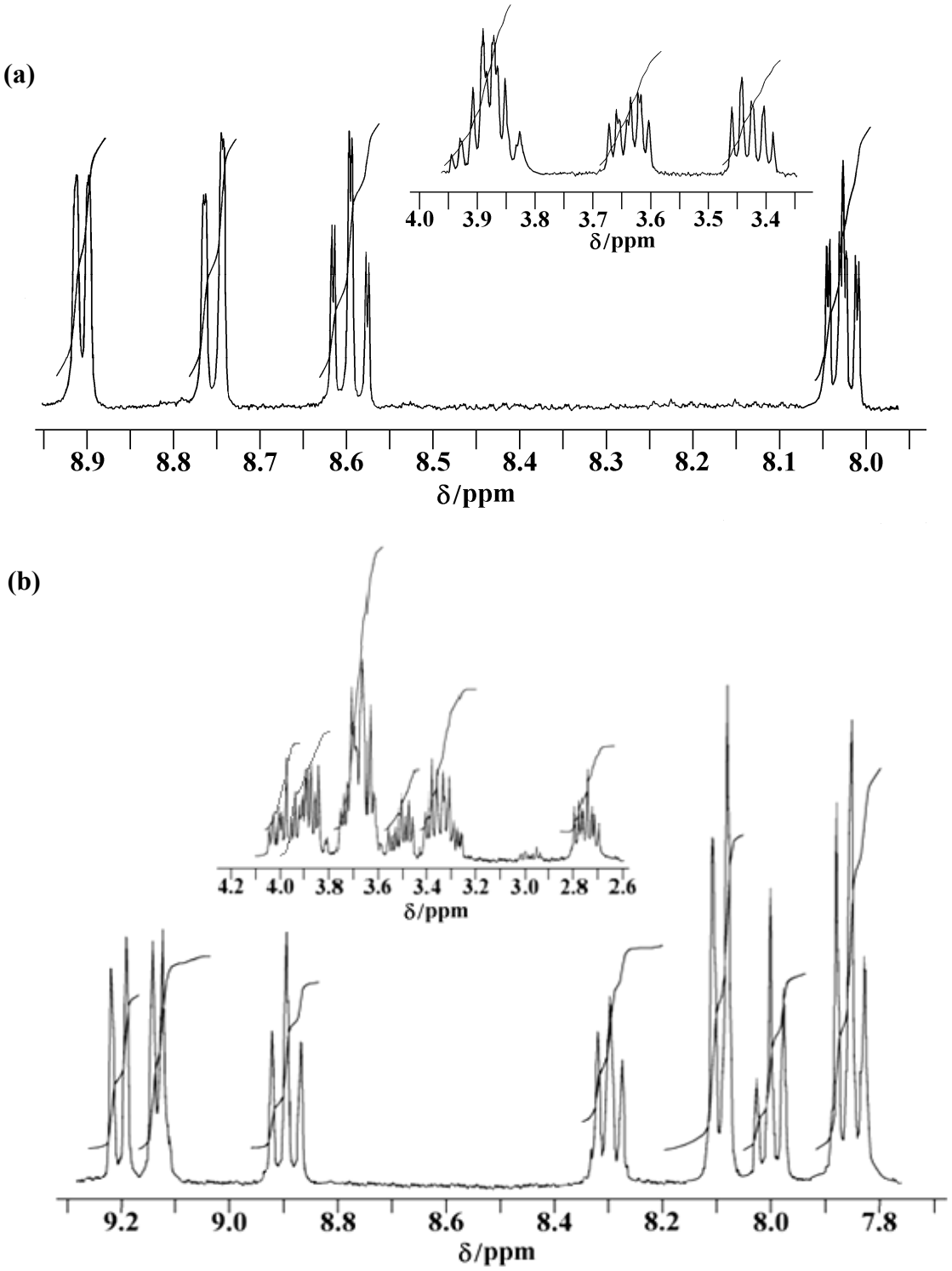

Fig. S5 ^{1}H NMR spectra in CD_3CN of (a) $[Ru^{II}([9]aneS_3)(bpy)(NO)]^{3+}$ ($\mathbf{4}^{3+}$) and (b) $[Ru^{II}([9]aneS_3)(pap)(NO)]^{3+}$ ($\mathbf{8}^{3+}$).

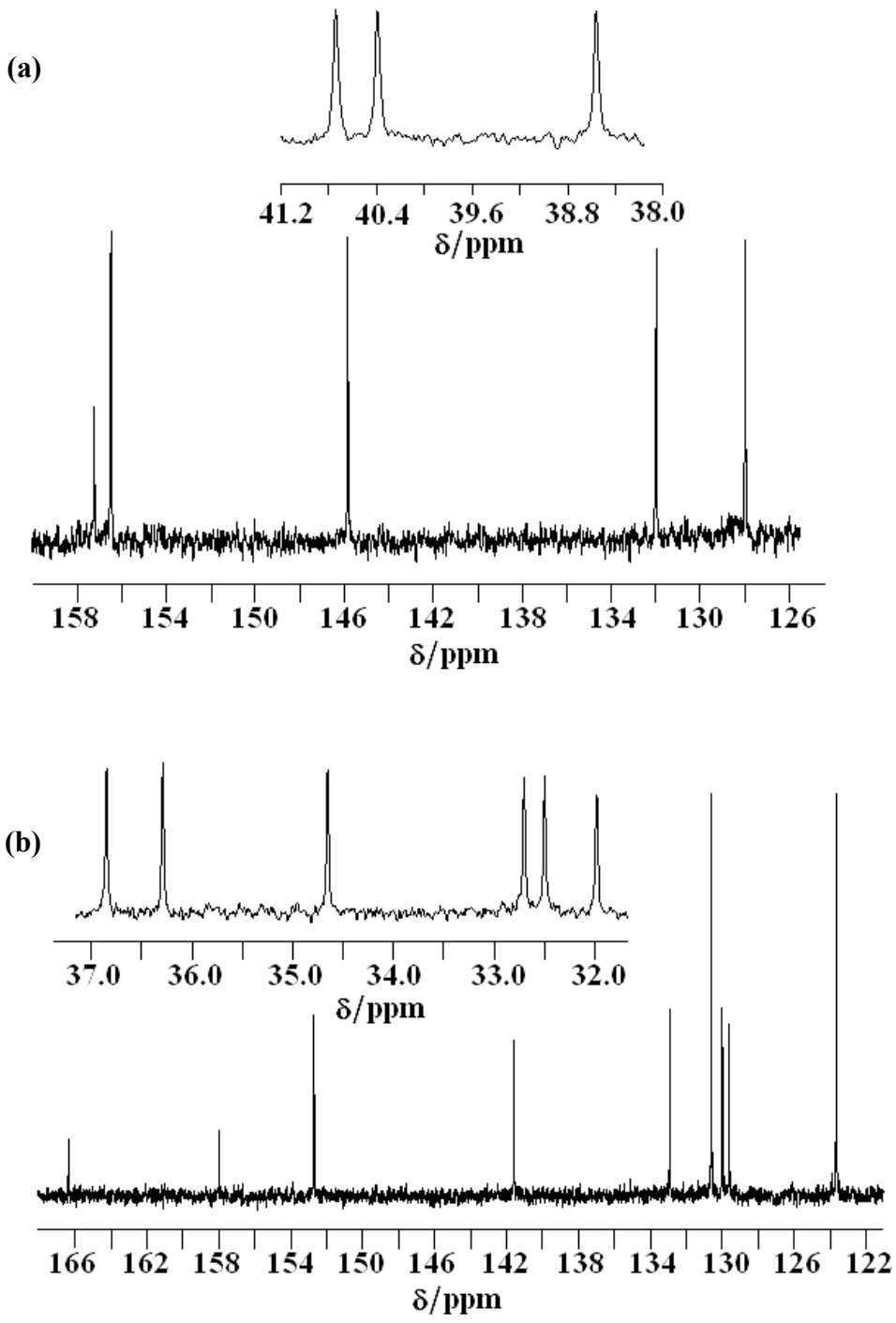

Fig. S6 ^{13}C NMR spectra in CD_3CN of (a) $[Ru^{II}([9]aneS_3)(bpy)(NO)]^{3+}$ ($\mathbf{4}^{3+}$) and (b) $[Ru^{II}([9]aneS_3)(pap)(NO)]^{3+}$ ($\mathbf{8}^{3+}$).

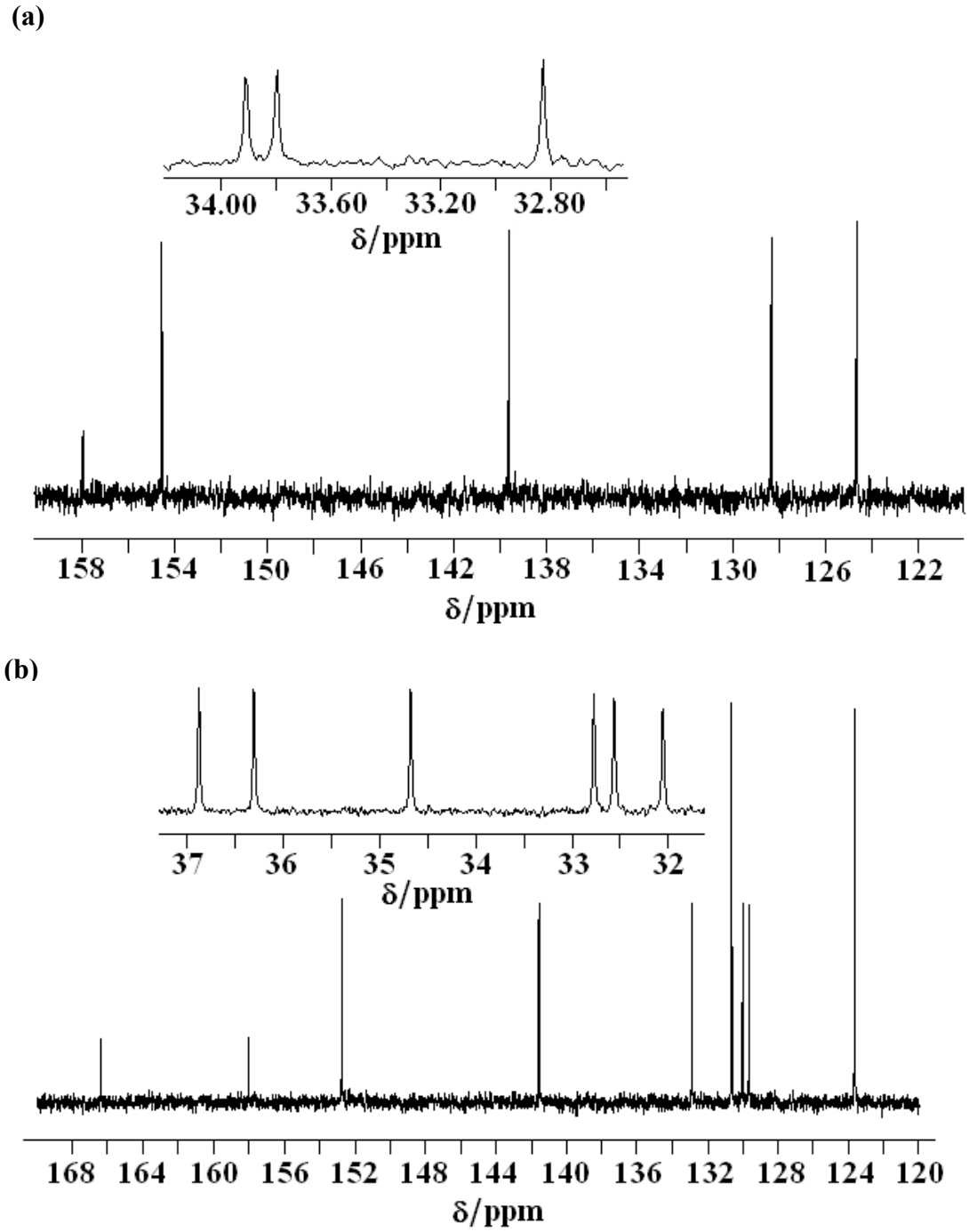

Fig. S7 ^{13}C NMR spectra in CD_3CN of (a) $[Ru^{II}([9]aneS_3)(bpy)(NO_2)]^+$ (**3**$^+$) and (b) $[Ru^{II}([9]aneS_3)(pap)(NO_2)]^+$ (**7**$^+$).

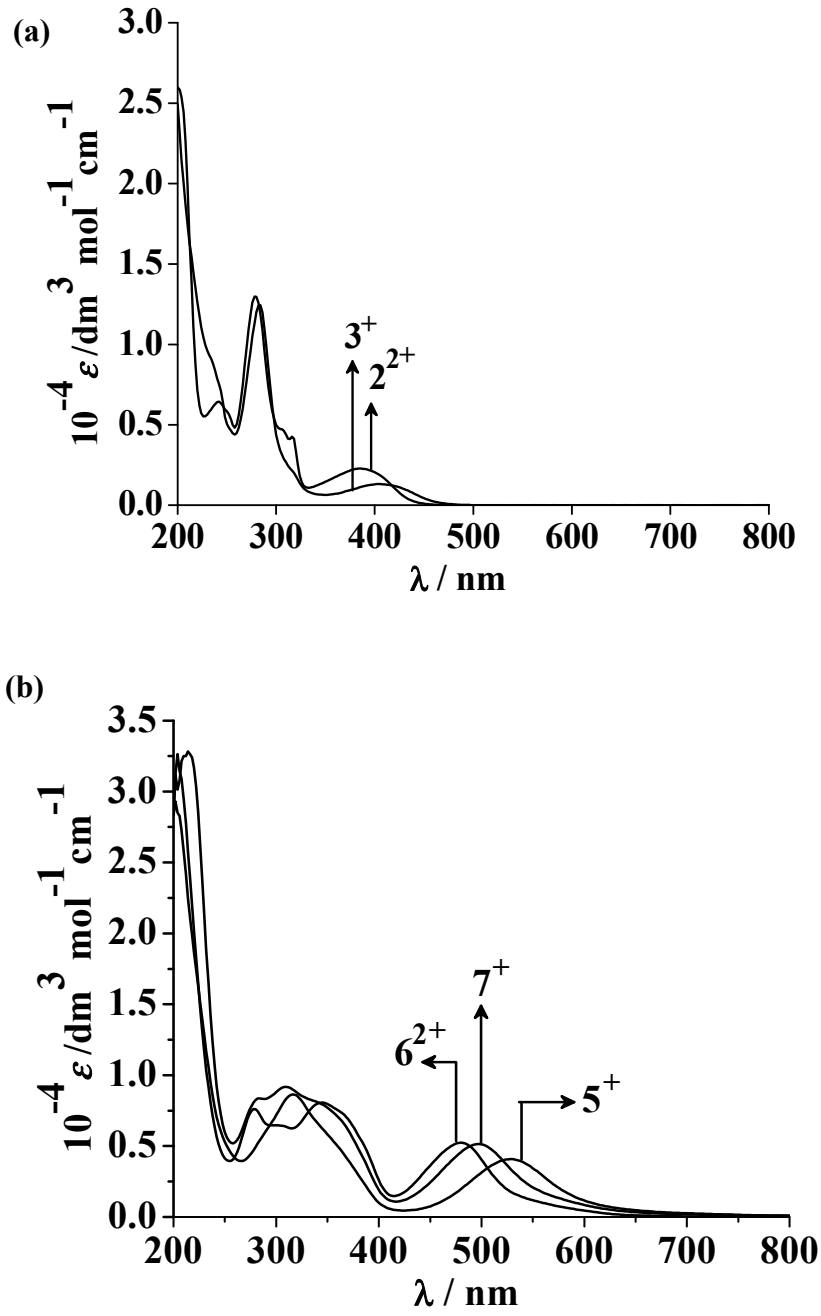

Fig. S8 Electronic spectra in CH_3CN of (a) $[Ru^{II}([9]aneS_3)(bpy)(CH_3CN)]^{2+}$ (**2**$^{2+}$), $[Ru^{II}([9]aneS_3)(bpy)(NO_2)]^{+}$ (**3**$^{+}$) and (b) $[Ru^{II}([9]aneS_3)(pap)(Cl)]^{+}$ (**5**$^{+}$), $[Ru^{II}([9]aneS_3)(pap)(CH_3CN)]^{2+}$ (**6**$^{2+}$), $[Ru^{II}([9]aneS_3)(pap)(NO_2)]^{+}$ (**7**$^{+}$).

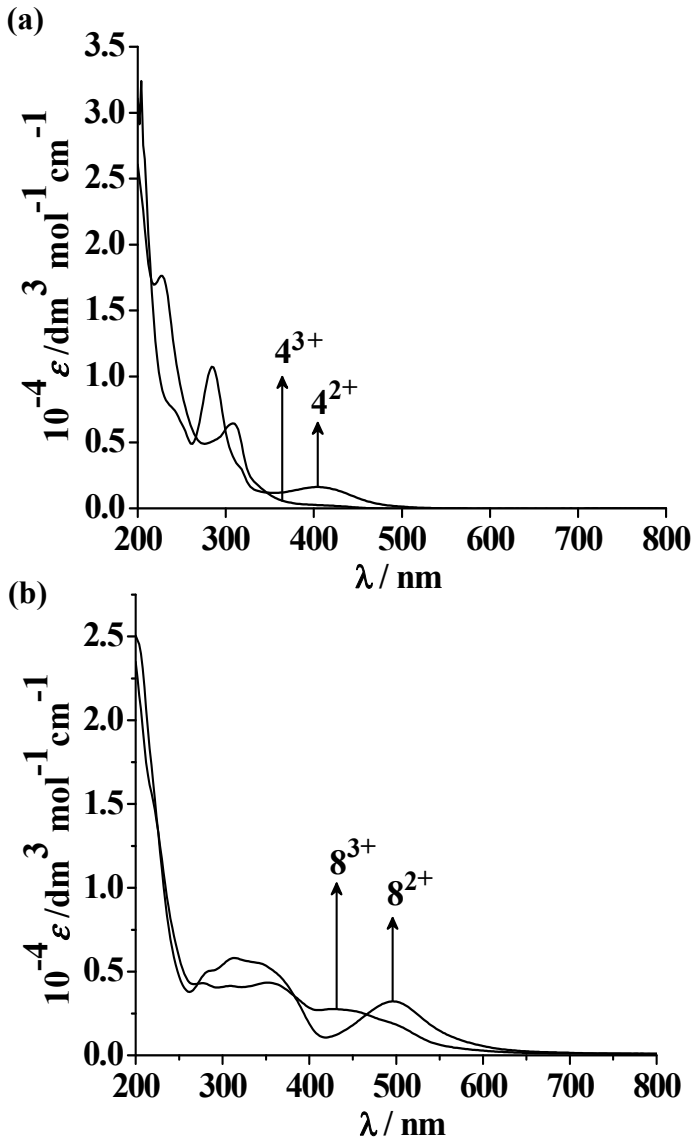

Fig. S9 Electronic spectra in CH_3CN of (a) $[Ru^{II}([9]aneS_3)(bpy)(NO)]^{3+}$ ($\mathbf{4}^{3+}$), $[Ru^{II}([9]aneS_3)(bpy)(NO)]^{2+}$ ($\mathbf{4}^{2+}$) and (b) $[Ru^{II}([9]aneS_3)(pap)(NO)]^{3+}$($\mathbf{8}^{3+}$), $[Ru^{II}([9]aneS_3)(pap)(NO)]^{2+}$ ($\mathbf{8}^{2+}$).

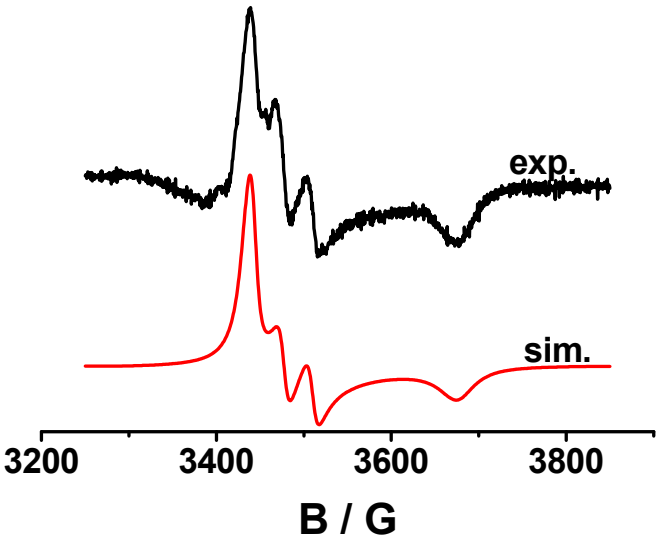

Fig. S10 EPR spectra of $[Ru^{II}([9]aneS_3)(bpy)(NO)]^{2+}$ ($\mathbf{4}^{2+}$) in CH_3CN at 110 K.